VIETNAM ACADEMY OF SCIENCE AND TECHNOLOGY

Vietnam Journal of MECHANICS

Volume 35 Number 4

ISSN 0866-7136

VN INDEX 12.666

4

2013

35th Anniversary

Vietnam Journal of Mechanics, VAST, Vol. 35, No. 4 (2013), pp. 299 – 311

CHANGE IN MODE SHAPE NODES OF MULTIPLE CRACKED BAR: II. THE NUMERICAL ANALYSIS

N. T. Khiem*, L. K. Toan, N. T. L. Khue
Institute of Mechanics, VAST, 18 Hoang Quoc Viet, Hanoi, Vietnam
*E-mail: ntkhiem@imech.ac.vn

Abstract. In this paper it is numerically analyzed the change in position of mode shape nodes induced by multiple cracks in bar that has been theoretically investigated in previous paper [1] of the authors. The focus is to analyze thoroughly dislocation of node located intermediately between two cracks in dependence upon the crack parameters without assumption on the smallness of crack.

Keywords: Multiple cracked bar, crack detection, mode shape nodes, vibration method, modal analysis.

1. INTRODUCTION

This paper is devoted to continue the study of change in node position induced by multiple cracks in bar by numerical examples. First, some theoretical aspects that were detailed in the previous paper are summarized to use for numerical computation. The emphasis is on the numerical investigating the case of double cracks and change in position of the node located between cracks. Two cases of boundary conditions: free-free and fixed-free ends are considered.

2. SUMMARIZED THEORETICAL ASPECTS

For an uniform bar with Young's modulus E, density ρ, cross section area A and length L that is assumed to be cracked at the locations $e_1, ..., e_n$, free longitudinal vibration is described by the equation

$$\Phi''(x) + \lambda^2\Phi(x) = 0,\ x \in (0,1),\ \lambda = \omega L/c_0,\ c_0 = \sqrt{E/\rho} \tag{1}$$

with given boundary conditions at both ends $x = 0, x = 1$ and the compatibility conditions at the crack positions

$$\Phi(e_j + 0) = \Phi(e_j - 0) + \gamma_j\Phi'(e_j),\ \gamma_j = EA/LK_j,\ j = 1, ..., n. \tag{2}$$

It was shown in previous paper [1] that general solution of Eqs. (1), (2) all over the bar length can be represented as

$$\Phi(x) = \Phi_0(x) + \sum_{j=1}^{n} \mu_j K(x - e_j, \lambda), \tag{3}$$

where $\Phi_0(x)$ is general solution of Eq. (1) satisfying the left end condition and

$$\mu_j = \gamma_j[\Phi_0'(e_j) + \sum_{k=1}^{n} \mu_k K'(e_j - e_k, \lambda)], j = 1, ..., n; \tag{4}$$

$$K(x,\lambda) = \begin{cases} 0, & x \le 0 \\ \cos\lambda x, & x \succ 0 \end{cases} \quad ; \quad K'(x,\lambda) = \begin{cases} 0, & x \le 0 \\ -\lambda \sin\lambda x, & x \succ 0 \end{cases} \tag{5}$$

Obviously, the solution $\Phi_0(x)$ can be represented as $\Phi_0(x) = \mathrm{C}L_0(x,\lambda)$, where C is a constant and $L_0(x,\lambda)$ called shape function is the solution of Eq. (1) satisfying the left boundary condition. For instance, in the case of general boundary condition $\alpha_0\Phi(0) + \beta_0\Phi'(0) = 0$ the shape function is $L_0(\lambda x) = \alpha_0 \sin\lambda x - \beta_0\lambda\cos\lambda x$. If the bar is fixed at the left end, $x = 0$, $L_0(x,\lambda) = \sin\lambda x$ and $L_0(x,\lambda) = \cos\lambda x$ for the free one. The constant C would be determined from the boundary condition at the right end $x = 1$ that can be expressed in the form $\alpha_1\Phi(1) + \beta_1\Phi'(1) = 0$. Substituting Eq. (3) with function $\Phi_0(x) = \mathrm{C}L_0(x,\lambda)$ into the boundary condition at the right end $x = 1$ leads to

$$\mathrm{C}[\alpha_1 L_0(1,\lambda) + \beta_1 L_0'(1,\lambda)] + \sum_{j=1}^{n} \mu_j[\alpha_1 K(1 - e_j, \lambda) + \beta_1 K'(1 - e_j, \lambda)] = 0$$

from that one gets

$$\mathrm{C} = -\,[1/D_0(\lambda)] \sum_{j=1}^{n} \mu_j K_1(e_j, \lambda); \tag{6}$$

$$D_0(\lambda) = \alpha_1 L_0(1,\lambda) + \beta_1 L_0'(1,\lambda); K_1(e_j,\lambda) = \alpha_1 K(1 - e_j,\lambda) + \beta_1 K'(1 - e_j,\lambda)$$

.

Using Eq. (6) the Eqs. (3) and (4) can be rewritten as

$$\Phi(x) = \sum_{j=1}^{n} \mu_j \alpha(x, e_j, \lambda)\,, \tag{7}$$

$$\alpha(x,e,\lambda) = [D_0(\lambda)K(x - e,\lambda) - K_1(e,\lambda)L_0(x,\lambda)]/D_0(\lambda) \tag{8}$$

and

$$[\mathbf{\Gamma}(\boldsymbol{\gamma})\mathbf{A}(\mathbf{e},\lambda) - D_0(\lambda)\mathbf{I}]\boldsymbol{\mu} = 0, \tag{9}$$

where

$$\boldsymbol{\mu} = (\mu_1, ..., \mu_n)^T, \boldsymbol{\gamma} = (\gamma_1, ..., \gamma_n)^T, \mathbf{e} = (e_1, ..., e_n)^T, \mathbf{\Gamma} = diag\{\gamma_1, ..., \gamma_n\};$$
$$\mathbf{A} = [a_{jk} = a(e_j, e_k, \lambda);\ j,k = 1, ..., n], \tag{10}$$
$$a(e_j, e_k, \lambda) = D_0(\lambda)K'(e_j - e_k,\lambda) - L_0'(e_j,\lambda)K_1(e_k,\lambda);\ j,k = 1, ..., n.$$

For existence of non-trivial vector $\boldsymbol{\mu}$ as a solution of Eq. (10), it must be satisfied the condition

$$D(\lambda, \mathbf{e}, \boldsymbol{\gamma}) \equiv \det[\mathbf{\Gamma}(\boldsymbol{\gamma})\mathbf{A}(\mathbf{e},\lambda) - D_0(\lambda)\mathbf{I}] = 0. \tag{11}$$

This is a new form of the frequency equation in axial vibration for multiple cracked bar [2]. Obviously, the latter equation is determined by the determinant of order identical to the number of cracks. Solving Eq. (11) with respect to λ results in so-called eigenvalues $\lambda_p, p = 1, 2, ...$ that relate to the natural frequencies $\omega_p, p = 1, 2, ...$ by the relationship $(\lambda_p/L)\sqrt{E/\rho} = \omega_p$. Each eigenvalue λ_p associates with a non-trivial solution of Eq. (13) that is so-called eigenvector μ_p of p-th mode. Thus the couple (λ_p, μ_p) enables to express the mode shape in the explicit form

$$\Phi_p(x) = \mathrm{C}_p \sum_{j=1}^{n} \mu_{pj} \alpha(x, e_j, \lambda_p)\,. \tag{12}$$

The constant C_p is introduced in the latter equation because the eigenvector μ_p determined as a solution of Eq. (13) should contain an arbitrary constant that can be determined by choosing a normality condition, for example, $\max\{\Phi_p(x)\} = 1$.

For a bar with a double crack the frequency Eq. (11) leads to

$$\begin{aligned} D_0(\lambda) + [\gamma_1 L_0'(e_1, \lambda) K_1(e_1, \lambda) + \gamma_2 L_0'(e_2, \lambda) K_1(e_2, \lambda)] + \\ + \gamma_1\gamma_2 L_0'(e_1, \lambda) K_1(e_2, \lambda) K'(e_2 - e_1, \lambda)] = 0. \end{aligned} \tag{13}$$

The expression (12) for mode shape now can be written as

$$\begin{aligned} \phi(x, \lambda) = \mathrm{C}[\mu_1 \alpha(x, e_1, \lambda) + \mu_2 \alpha(x, e_2, \lambda)] = \mathrm{C}\{L_0(x, \lambda) + \gamma_1 L_0'(e_1, \lambda) K(x - e_1) + \\ + \gamma_2 [L_0'(e_2, \lambda) + \gamma_1 L_0'(e_1, \lambda) K'(e_2 - e_1, \lambda)] K(x - e_2)\}, \end{aligned}$$

that leads the mode shape node of the double cracked bar to be determined as root of the equation

$$L_0(x, \lambda) + \gamma_1 L_0'(e_1, \lambda) K(x - e_1) + \gamma_2 [L_0'(e_2, \lambda) + \gamma_1 L_0'(e_1, \lambda) K'(e_2 - e_1, \lambda)] K(x - e_2) = 0,$$

or

$$L_0(x, \lambda) = 0, \quad 0 \prec x \leq e_1; \tag{14}$$

$$L_1(x, \lambda) \equiv L_0(x, \lambda) + \gamma_1 L_0'(e_1, \lambda) \cos\lambda(x - e_1) = 0, \ e_1 \prec x \leq e_2; \tag{15}$$

$$\begin{aligned} L_2(x, \lambda) \equiv L_1(x, \lambda) + \gamma_2 [L_0'(e_2, \lambda) + \gamma_1 L_0'(e_1, \lambda) K'(e_2 - e_1, \lambda)] \cos\lambda(x - e_2) = 0, \\ e_2 \prec x \prec 1. \end{aligned} \tag{16}$$

In the case of *free-free bar*, when $L_0(x, \lambda) = \cos\lambda x$, the frequency equation is

$$\begin{aligned} \sin\lambda - \lambda[\gamma_1 \sin\lambda e_1 \sin\lambda(1 - e_1) + \gamma_2 \sin\lambda e_2 \sin\lambda(1 - e_2)] + \\ + \lambda^2 \gamma_1\gamma_2 \sin\lambda e_1 \sin\lambda(e_2 - e_1) \sin\lambda(1 - e_2) = 0. \end{aligned} \tag{17}$$

The system of Eqs. (14), (15), (16) is reduced to

$$\cos\lambda_k x = 0, \quad 0 \prec x \leq e_1; \tag{18}$$

$$\cos\lambda_k x - \gamma_1 \lambda_k \sin\lambda_k e_1 \cos\lambda_k (x - e_1) = 0, \ e_1 \prec x \leq e_2; \tag{19}$$

$$\begin{aligned} \cos\lambda_k x - \gamma_1 \lambda_k \sin\lambda_k e_1 \cos\lambda(x - e_1) - \gamma_2 \lambda_k [\sin\lambda_k e_2 - \\ - \gamma_1 \lambda_k \sin\lambda_k e_1 \sin\lambda_k (e_2 - e_1)] \cos\lambda(x - e_2) = 0, \ e_2 \prec x \prec 1. \end{aligned} \tag{20}$$

Analytical solution of Eqs. (18), (19) has been obtained in the previous paper, it remains Eq. (19) rewritten as

$$\tan\lambda_k^0 \theta_k = \frac{\lambda_k \gamma_1 \sin^2 \lambda_k e_1}{1 - \lambda_k \gamma_1 \sin\lambda_k e_1 \cos\lambda_k e_1}, \ \ \theta_k \in (\Delta_1, \Delta_2), \tag{21}$$

where $x = \lambda_k^0(x_{kn}^0 - \theta_k)/\lambda_k$ and $\Delta_1 = x_{kn}^0 - \lambda_k e_2/\lambda_k^0$; $\Delta_2 = x_{kn}^0 - \lambda_k e_1/\lambda_k^0$ that has to be numerically solved. Owning solution $\hat{\theta}_k$ of Eq. (21) the mode shape node determined can be calculated as $x_{kn} = \lambda_k^0(x_{kn}^0 - \hat{\theta}_k)/\lambda_k$, consequently, dislocation of the node from the generic one is

$$\delta x_{kn} \equiv x_{kn} - x_{kn}^0 = (\delta\lambda_k/\lambda_k)x_{kn}^0 - (\lambda_k^0/\lambda_k)\hat{\theta}_k. \tag{22}$$

where $\delta\lambda_k = \lambda_k^0 - \lambda_k$.

If the *bar is fixed at both the ends*, $L_0(x,\lambda) = \sin\lambda x$, the frequency and node are sought from the equations

$$\begin{aligned}\sin\lambda + \lambda[\gamma_1 \cos\lambda e_1 \cos\lambda(1-e_1) + \gamma_2 \cos\lambda e_2 \cos\lambda(1-e_2)] - \\ -\lambda^2\gamma_1\gamma_2 \cos\lambda e_1 \sin\lambda(e_2-e_1)\cos\lambda(1-e_2) = 0\end{aligned} \tag{23}$$

and one obtains equation similarly to the Eq. (21) as

$$\tan\lambda_k^0\theta_k = \frac{\lambda_k\gamma_1\cos^2\lambda_k e_1}{1+\lambda_k\gamma_1\sin\lambda_k e_1\cos\lambda_k e_1}, \;\; \theta_k \in (\Delta_1, \Delta_2) \tag{24}$$

with $\Delta_1 = x_{kn}^0 - \lambda_k e_2/\lambda_k^0$; $\Delta_2 = x_{kn}^0 - \lambda_k e_1/\lambda_k^0$.

For the *bar with fixed-free ends*, the characteristic equation is

$$\begin{aligned}\cos\lambda - \lambda[\gamma_1 \cos\lambda e_1 \sin\lambda(1-e_1) + \gamma_2 \cos\lambda e_2 \sin\lambda(1-e_2)] + \\ +\lambda^2\gamma_1\gamma_2 \cos\lambda e_1 \sin\lambda(e_2-e_1)\sin\lambda(1-e_2) = 0.\end{aligned} \tag{25}$$

Though the characteristic Eq. (25) is different from the ones for the previous cases, the equations for the mode shape node in this case of boundary condition give solutions identical to those of the fixed-fixed bar.

3. NUMERICAL RESULTS

To investigate effect of cracks on the shift of the intermediate node the dislocation of node is computed based on the numerical solution of Eqs. (21) and (24) in dependence on different combinations of position and depth of two cracks. The Eq. (21) represents the bar with free ends and Eq. (24) - the cantilevered bar. For simplicity, the crack located on the left (right) of a node is called left (right) crack and only the modes that have single and double node are considered. The positive displacement of a node implies that it moves to the right and negative displacement - to the left.

First scenario is examined for cracks of equal depth and varying positions in both sides of generic node with purpose to highlight influence of crack position on the node dislocation. In the second scenario the contours of zero displacement of nodes are plotted in the plane of position and depth of left crack with different fixed parameters of right crack. This task is accomplished to reveal influence of cracks depth on the direction by which a node move due to the cracks. Numerical results are shown in Figs. 1-12 that allow for making the following discussion.

For the *bar with free ends*, single node at 0.5 moves toward the crack that is more close to it if the cracks have the same depth. It would move toward farther crack only if depth of the crack exceeds that of other one. Absolute displacement of the single node increases monotonically with reduction of distance from node to closer crack. The node

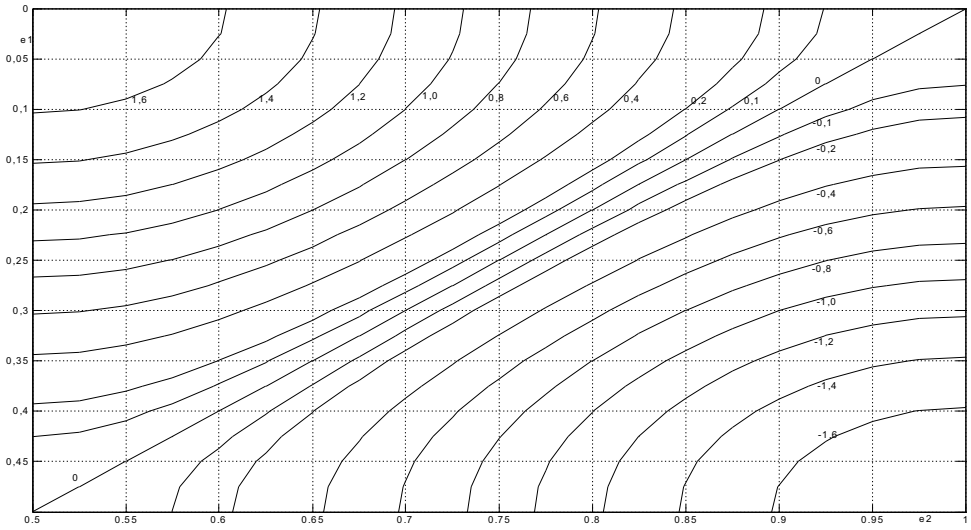

Fig. 1. The free-free bar: contours for dislocation of single node (first mode) versus positions of cracks of equal depth a/h = 30%

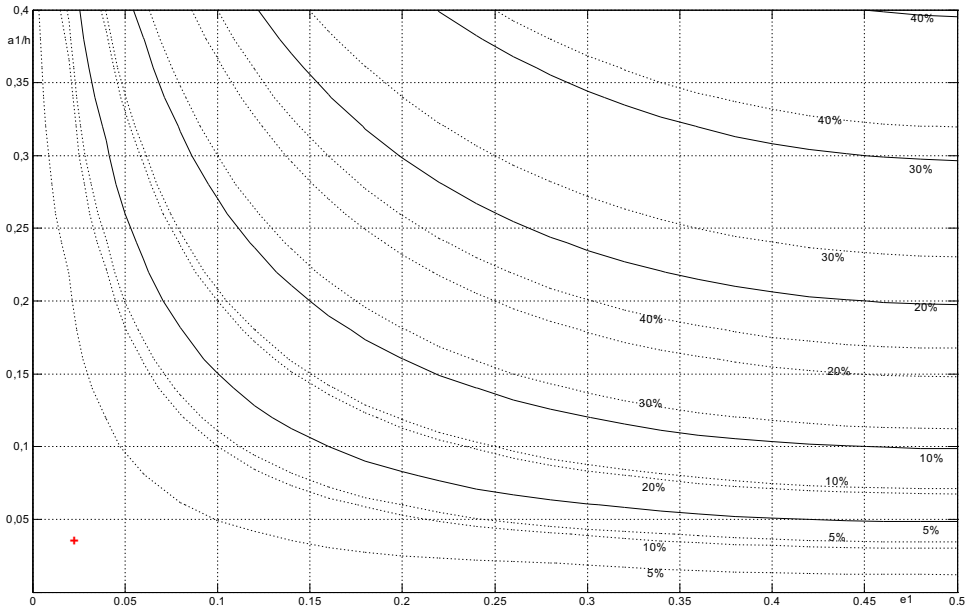

Fig. 2. The free-free bar: contours for zero displacement of single node (first mode) versus position and depth of the left crack in different depth from 5% – 40% of the right crack at positions 0.55 (solid); 0.75(dash dot) and 0.9 (dot)

does not change its position for the cracks of equal depth located at the same distance from both sides of the node, see Figs. 1, 2.

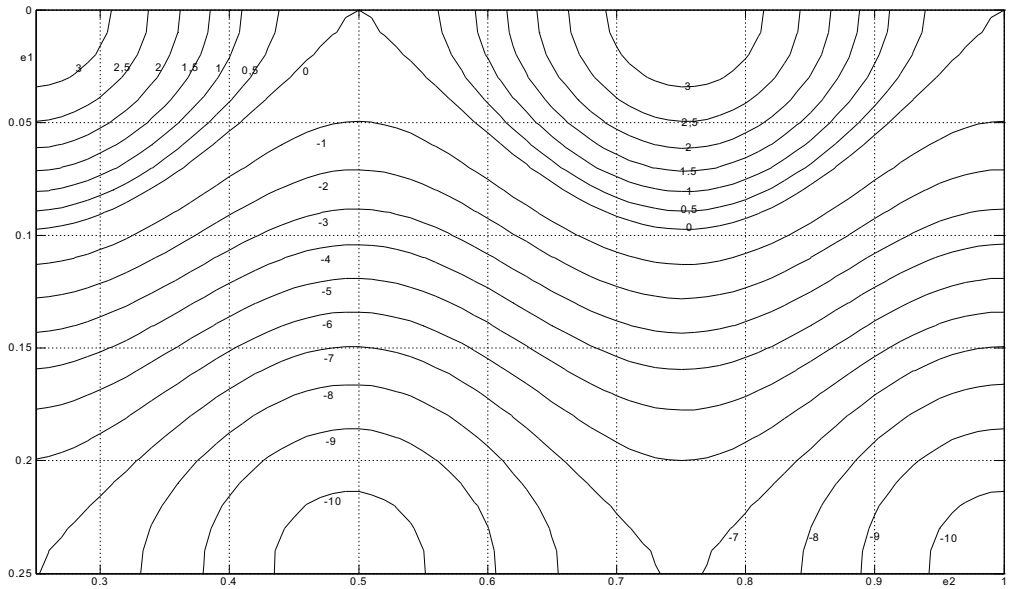

Fig. 3. The free-free bar: contours for dislocation of first node (second mode) versus positions of cracks of equal depth a/h = 30%

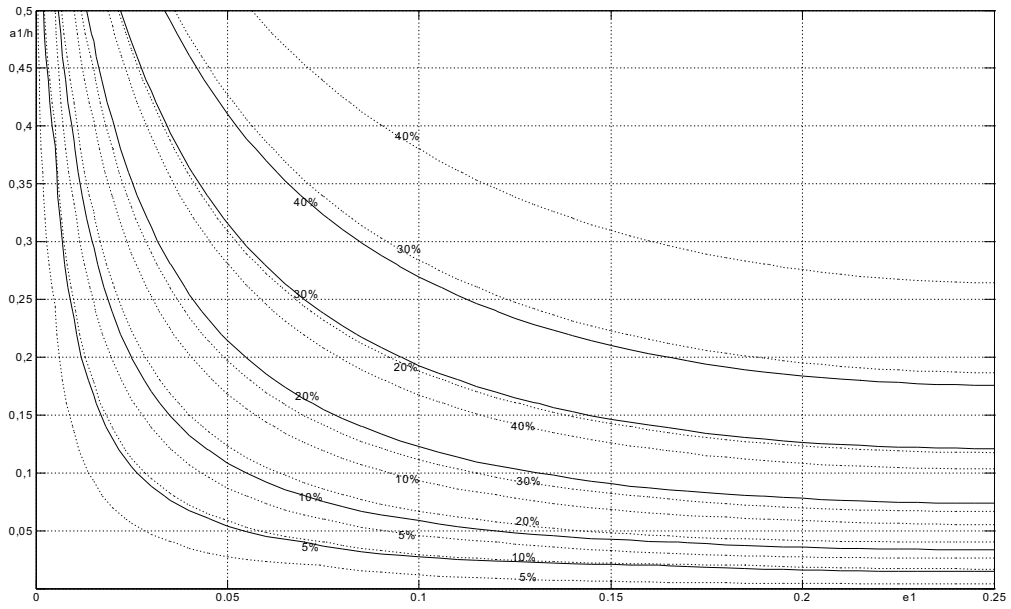

Fig. 4. The free-free bar: contours for zero displacement of first node (second mode) versus position and depth of the left crack in different depth 5% - 40% of the right crack at positions 0.4 (solid); 0.7 (dash dot) and 0.95 (dot)

It is observed more complicated behavior of nodes of second mode that has two nodes, the first is at 0.25 and the second one at 0.75, and one crack-unaffected point (ICP) at the middle of bar (0.5), see Tab. 1 [1]. Namely, it is apparent from Fig. 3 that in the case when the right crack is positioned in the segments from the node (0.25) to the ICP (0.5) and from second node (0.75) to the right end of bar the first node behaviors almost similarly to that is discussed above for the single node. The difference is only that zero displacement contour shifts to the left end of bar, perhaps, because the left end is a node and the middle is a ICP of the bar (no symmetry). For the right crack located in the segment from the ICP to the second node behavior of the first node is symmetrical about the axes $e_2 = 0.5$ and $e_2 = 0.75$ to its behavior in mentioned above two segments. This allows making a conclusion that for a given displacement of the first node it can be found

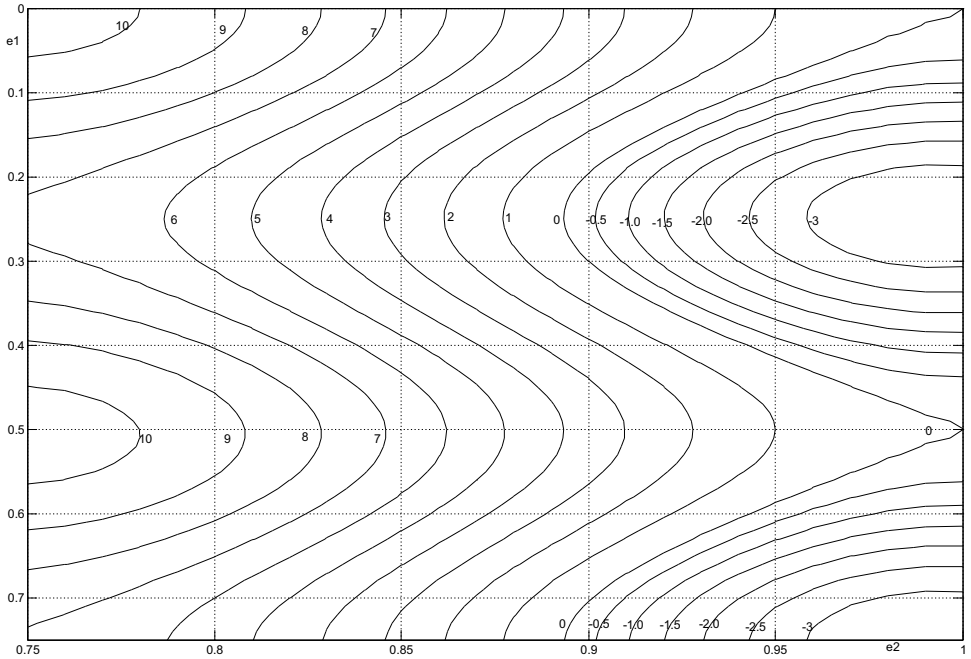

Fig. 5. The free-free bar: contours for dislocation of second node versus positions of cracks of equal depth a/h = 30%

one position preceding the node for the left crack and three positions belonging to three bar segment (0.25, 0.5); (0.5, 0.75) and (0.75, 1) respectively for the right crack. Otherwise speaking, the right crack at three positions symmetrical about the ICP, 0.5, and second node, 0.75, causes the same displacement of the first node. Moreover, the first node moves toward the left crack located from point 0.1 to the node (0.25) for arbitrary positions of the right crack. It may move to the right only for the position of left crack less than 0.1. The contour of zero displacement for the first node exists and is almost unchanged regarding to the crack depth. The negative and positive displacement domains for the first node versus position and depth of the left crack in different magnitudes of the right crack are shown in Fig. 4 that is similar to Fig. 2 for the single node. A little difference observed

between the Figures shows again the fact that a node can move toward the closer crack of less depth.

The contours for dislocation of second node for equal crack depth plotted in the plane (e_1, e_2) are shown in Fig. 5. It is easily to verify that Fig. 5 can be exactly obtained from Fig. 3 for the first node by the replacement of variables $e_1 = 1 - e_2'$; $e_2 = 1 - e_1'$. Therefore, a discussion similar to that has been made above for the first node can be simply conducted with taking account of the change in crack positions. However, zero displacement contours for the second node shown in Fig. 6 are considerably different from those for the first node. Namely, every contour for zero displacement is undetermined at the ICP, 0.5, and has two minimums at the two nodes (0.25 and 0.75). The uncertainty indicates that the left crack appeared at the ICP makes no effect on the second node. On the other hand, the minimum points of the contours say about positions the left crack at which makes largest effect on the second node. This exhibits the importance of positions for generic node and ICP in the representation of node shift caused by multiple cracks.

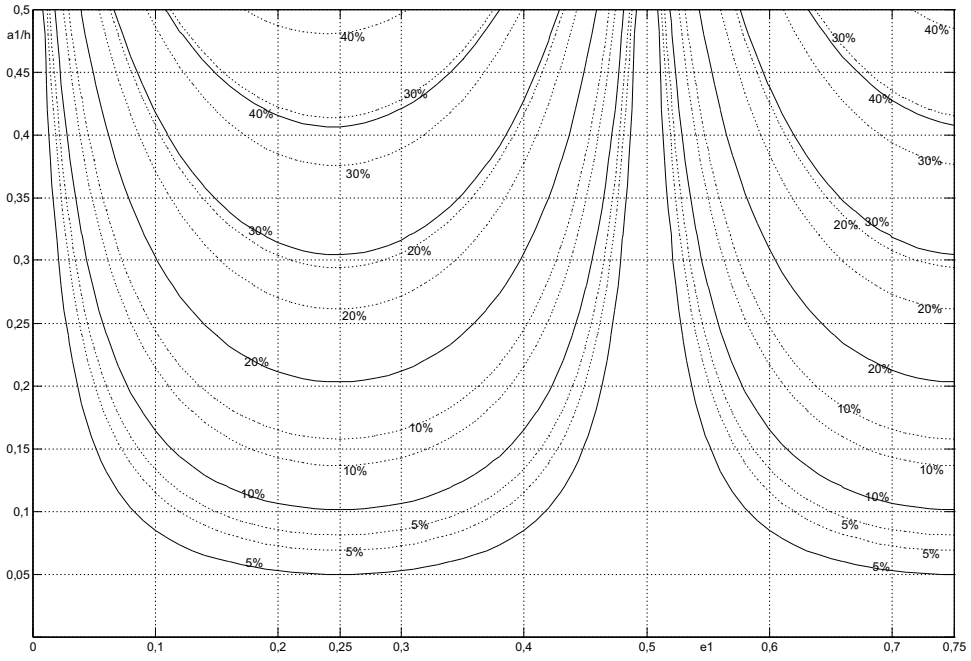

Fig. 6. The free-free bar: contours of zero displacement of second node (second mode) versus position and depth of the left crack in different depth from 5% – 40% of the right crack at positions 0.8 (solid); 0.85 (dash dot) and 0.9 (dot)

In the case of *cantilevered bar*, single node exists at the position 2/3 for second mode that has also a single ICP at the position 1/3. The third mode has two generic nodes 0.4 (the first) and 0.8 (the second) and two ICPs at 0.2 and 0.6 respectively. The contours for various dislocation of the single node given in Fig. 7 show that all the contours have the same axis of symmetry $e_1 = 1/3$ crossing the single ICP, the middle of the segment from left end to the node (0, 2/3). The symmetry points out that it can be found one position

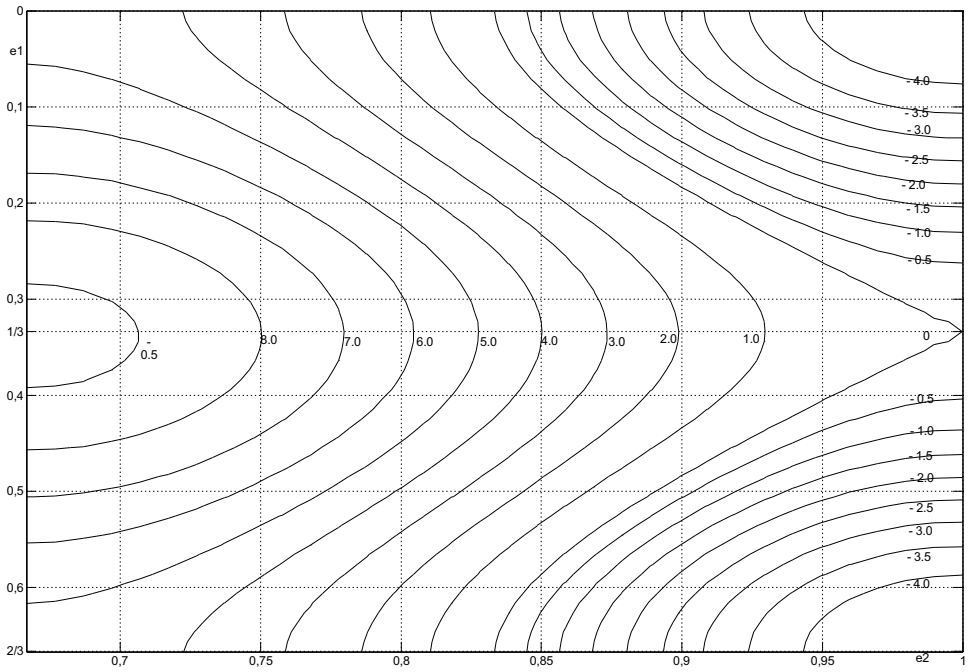

Fig. 7. The cantilever bar: contours for dislocation of single node (second mode), 2/3, versus positions of cracks of equal depth $a/h = 30\%$

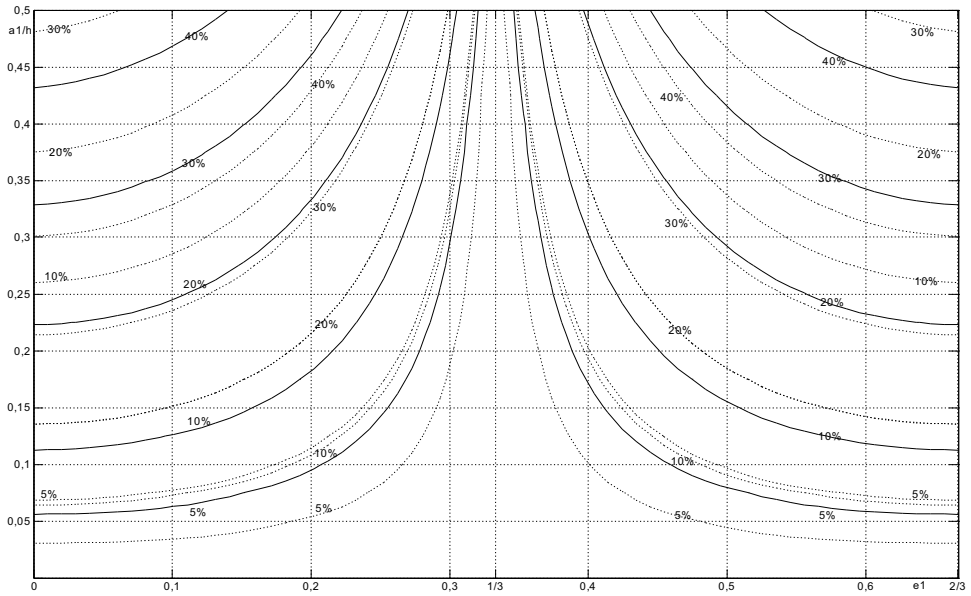

Fig. 8. The cantilever bar: contours for zero displacement of single node (second mode) versus position and depth of the left crack in different depth from 5 - 40% of the right crack at positions 0.7(dash dot); 0.8 (solid) and 0.9 (dot)

of the right crack and two symmetrical positions of the left crack for a given displacement of the node. Furthermore, the node cannot moves to the left if position of the right crack is less than 0.83 for wherever occurred the left crack of the same depth. The positive displacement of single node increases monotonically as the right crack approaching to the node. The negative displacement domain of single node consists of two separated small parts at the right corners enclosed by contour of zero displacement. The symmetry is observed more apparently also in Fig. 8 where there are shown various contours for zero displacement of the node plotted versus the left crack parameters for the right crack with depth from 5% to 40% at three positions 0.7, 0.8 and 0.9. It can be noted from the latter figure that effect of the left crack on the dislocation of the single node becomes more significant when the crack is more close to the left end and the node.

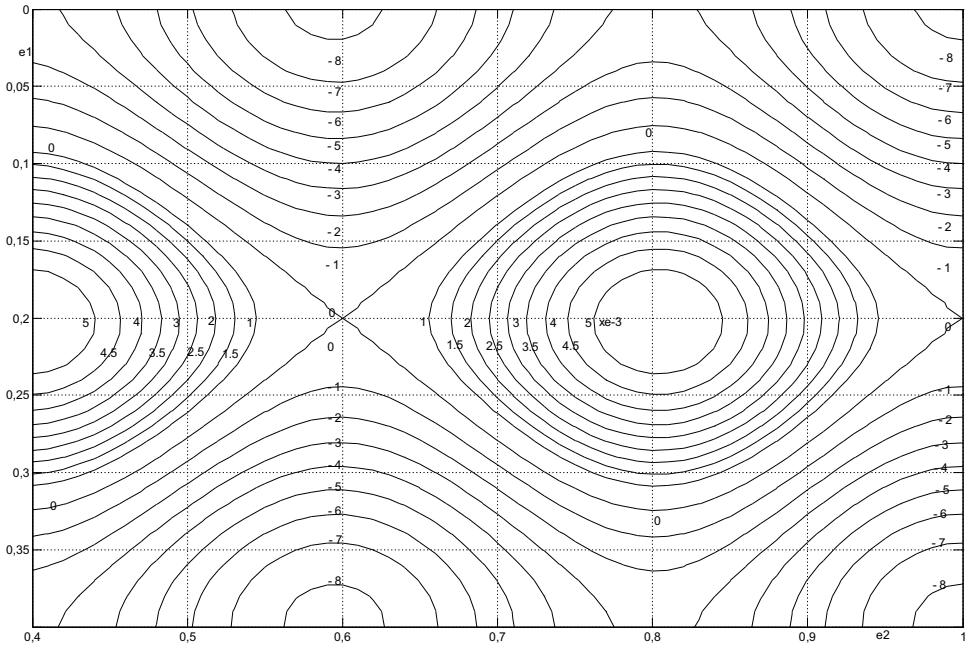

Fig. 9. The cantilever bar: contours for dislocation of first node 0.4 (third mode) versus positions of cracks with equal depth a/h = 30%

Behavior of double node for the third mode of cantilever bar is presented in Figs. 9-12. The contours for dislocation of the first node, 0.4, given in Figs. 9, 10 show that all the contours have one axis of symmetry, $e_1 = 0.2$ crossing the first ICP. So that one can find two positions for the left crack and one position for the right crack that make the same shift of the first node. The node cannot move to the right if the left crack appeared at positions less than 0.075 and more than 0.325 for the right crack appeared wherever in the segment (0.4, 1.0). This implies also that the first node may move to the right if the left crack appears in the segment (0.075, 0.325). The behavior of the first node for the right crack appeared in the segments (0.4, 0.6) and (0.8, 1.0) is fully similar and dislocation of the node for the right crack located between 0.6 and 0.8 is symmetrical to that mentioned

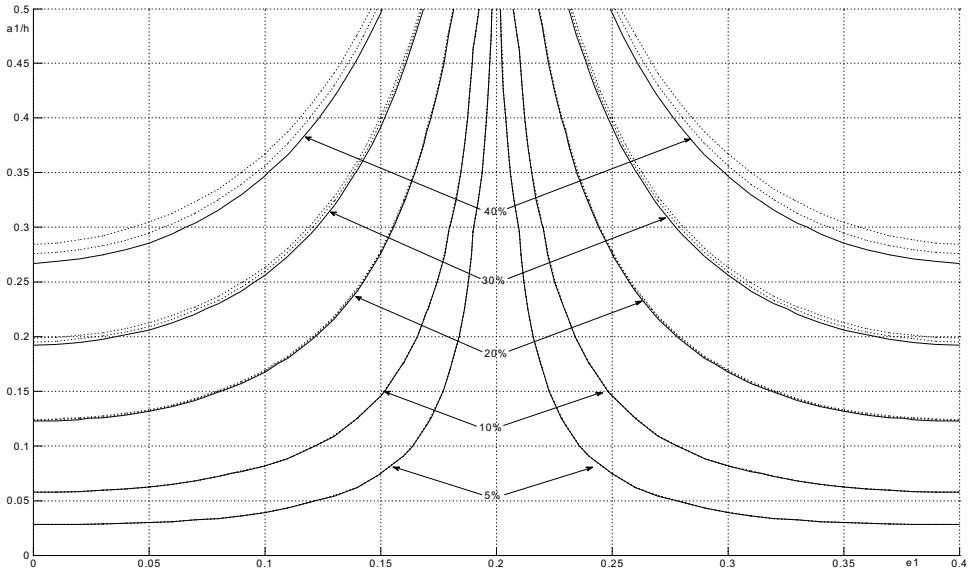

Fig. 10. The cantilever bar: contours for zero displacement of first node 0.4 (third mode) versus position and depth of the left crack in different depth from 5% – 40% of for the right crack at positions 0.5 (solid); 0.7 (dash dot) and 0.9 (dot)

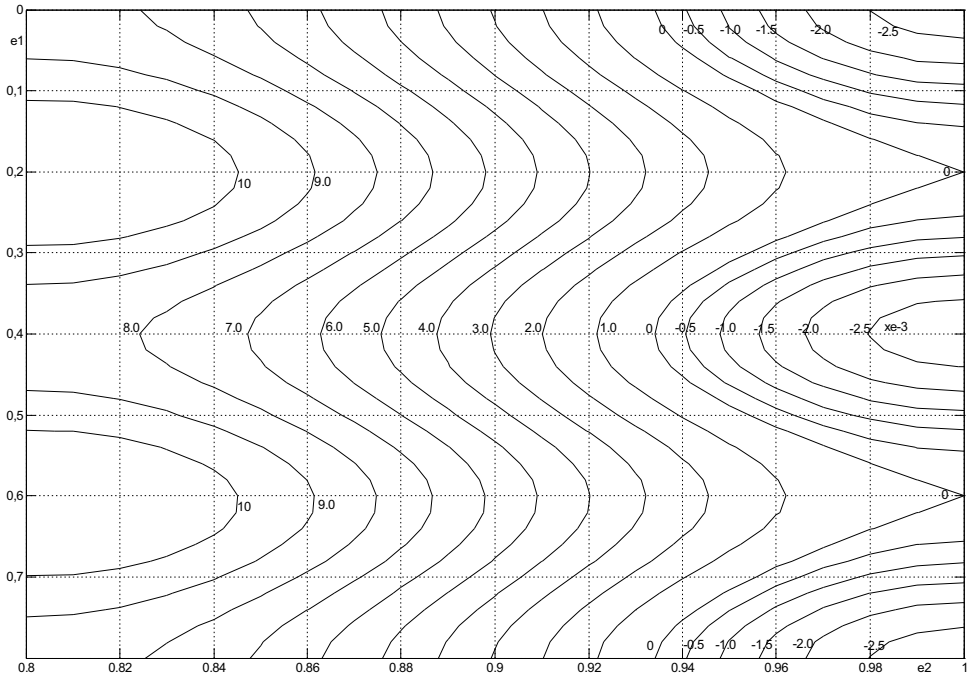

Fig. 11. The cantilever bar: contours for dislocation of second node 0.8 (third mode) versus positions of cracks of equal depth $a/h = 30\%$

previously. Consequently, for a given position of the left crack and displacement of the first node it can be found three positions for the right crack. The node is really unmoved if both the cracks coincide with the ICPs, 0.2 and 0.6. The typical differences observed in the figures are intersection of zero displacement contour and existence of closed contours of positive displacement and effect of the left crack becomes more significant as it approaching to the fixed end of bar.

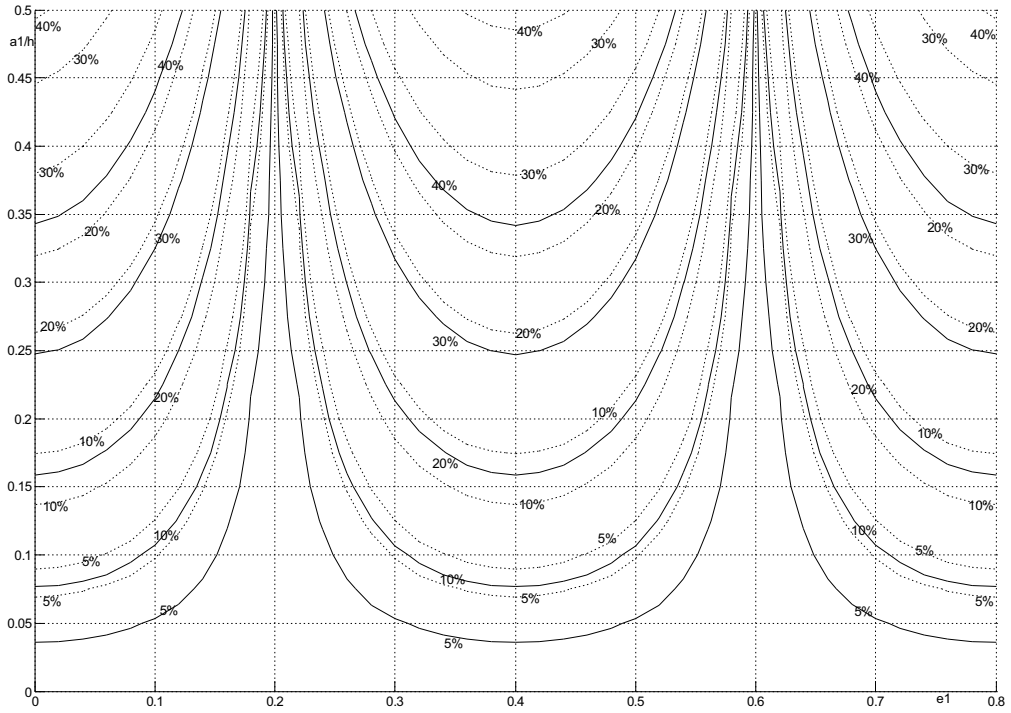

Fig. 12. The Cantilever bar: contours for zero displacement of second node 0.8 (third mode) versus position and depth of the left crack in different depth from 5% - 40% of the right crack at positions 0.85 (solid); 0.9 (dash dot) and 0.95 (dot)

The contours for dislocation of second node (0.8) shown in Figs. 11, 12 remain totally symmetrical about the axis $e_1 = 0.4$ and two the symmetrical portions in turn have also local axes of symmetry $e_1 = 0.2$, $e_1 = 0.6$ crossing the ICPs of this mode. These symmetries lead to the fact that there are four positions of the left crack associated with one value of node displacement and a position of the right crack. Moreover, the negative displacement domain exists only for the right crack located at the positions exceeding 0.935 and consists of three separated parts connected each to other by the ICPs 0.2 and 0.6. In this case, the most affected positions of the left crack for the second are fixed end and two generic nodes of the bar, see Fig. 12.

4. CONCLUSIONS

The obtained numerical results show that the intermediate single node is generally arranged to move toward the crack that is closer to it. It may move toward farther crack if depth of the crack is larger than that of the rest. In the case of multiple nodes, the effect of a crack on dislocation of a node becomes more significant if the crack approaches to the other node and the effect is eliminated when the crack occurred at an inactive crack point. Multiple cracks at different positions may produce the same change in a node position, but the different positions of multiple cracks are related each to other by symmetry about certain axes. There exists always an arrangement of two cracks that can maintain an intermediate node unmovable.

ACKNOWLEDGEMENT

This work has been completed with the financial supports from NAFOSTED of Vietnam under Grant No. 107.04.12.09, for which the authors are sincerely thankful.

REFERENCES

[1] N. T. Khiem, L. K. Toan, N. T. L. Khue, Change in mode shape nodes of multiple cracked bar: I. The theoretical study, *Vietnam Journal of Mechanics*, **35**(3), (2013), pp. 175-188.

[2] Ruotolo R., Surace C., Natural frequencies of a bar with multiple cracks, *Journal of Sound and Vibration*, **272**, (2004), pp. 301–316.

Received October 16, 2012

VIETNAM ACADEMY OF SCIENCE AND TECHNOLOGY
VIETNAM JOURNAL OF MECHANICS VOLUME 35, N. 4, 2013

CONTENTS

Pages